2.10. Statistical analyses

Statistical significance was determined using ANOVA followed by Student's *t*-test or Dunnett's test. Repeated measures two-way ANOVA was used for the statistical analysis for the rotarod test. *P* values less than 0.05 were considered to be significant.

3. Results

3.1. GL binding to HMGB1

The BIAcore sensograms of GL to immobilized HMGB1 showed a rapid increase in response units (RU) indicating binding of GL to the immobilized HMGB1 on the chip followed by a decrease of RU resulting from the dissociation of binding molecules upon washing. The binding of GL to HMGB1 was concentration-dependent (Fig. 1A). The equilibrium dissociation constant (Kd) was determined to be 4.03 μM. On the other hand, the GL binding to immobilized sRAGE was minimal (Fig. 1A).

The in vitro binding assay of HMGB1 to sRAGE showed that GL could block HMGB1 binding to sRAGE concentration-dependently (Fig. 1B). The IC50 value of GL was estimated to be 6 μM from the inhibition curve. Thus these results suggested that GL inhibited the interaction between HMGB1 and RAGE by binding to HMGB1.

3.2. Translocation of HMGB1 at the injured site and effect of GL

In the fluid percussion-induced injury model, translocation of HMGB1 from the nuclei to the cytosol was remarkable in MAP2-

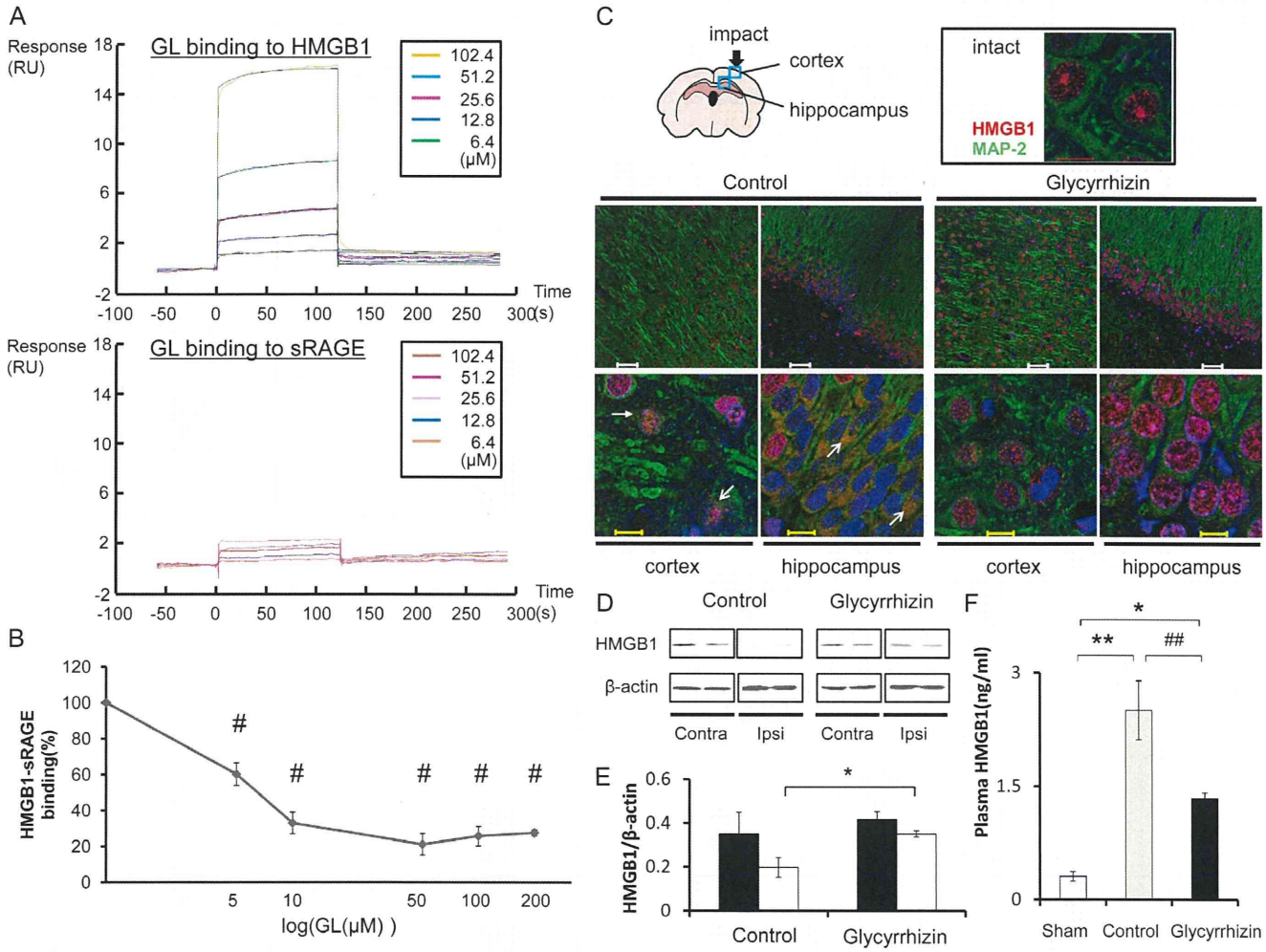

Fig. 1. (A) GL binding to HMGB1 in vitro. Recombinant human HMGB1 (40 μg/ml) was immobilized on a CM5 BIAcore chip and different concentrations of GL were flowed at time zero for 120 s. Surface plasmon resonance (BIAcore) showed a rapid increase in RU indicating binding of GL to the immobilized HMGB1. The Kd for GL binding to HMGB1 was determined to be 4.0 μM. Similarly, recombinant human sRAGE (53 μg/ml) was immobilized on a CM5 BIAcore chip and the binding of GL to sRAGE was determined. The GL binding to sRAGE was minimal. (B) The effect of GL on HMGB1–RAGE interaction in vitro. An in vitro binding assay of HMGB1 to sRAGE in the presence of different concentrations of GL to sRAGE was performed. The IC_{50} value of GL was estimated to be 6 μM from the inhibition curve. The results are expressed as the mean ± SEM of 3 wells. $^{\#}P < 0.05$ compared with the control value in the absence of GL. (C) Translocation of HMGB1 in neurons in the rat cortex and hippocampus in the ipsilateral hemisphere after TBI. Five minutes after fluid percussion injury on the right temporal cortex (top panel), the rats received an intravenous injection of GL (4.0 mg/kg) or control vehicle, and at 6 h after percussion the brains were fixed. The coronal brain sections were double-immunostained with anti-HMGB1 and anti-MAP-2 antibodies, followed by AlexaFluor 555-labeled and AlexaFluor 488-labeled secondary antibodies, respectively. Nuclei were stained by DAPI. The indicated areas from cerebral cortex and hippocampus CA1 were shown both at lower (upper panels) and higher (lower panels) magnifications. White arrows indicate the HMGB1-immunoreactivities in the extranuclear space. Scale bars: 50 μm (white) and 5 μm (yellow). (D) Decrease in HMGB1 levels in the TBI region. Brain samples from both sides of the cerebral cortex (3 mm square) were collected 24 h after injury for western blotting. β-actin was used as the internal control. (E) Quantitative analysis was performed using NIH Image J software. Results are expressed as the mean ± SEM of 5 rats. $^{*}P < 0.05$ compared with the control rats. (F) Plasma levels of HMGB1 were determined by ELISA in rats with TBI 6 h after injury. Results are expressed as the mean ± SEM of 10 rats. $^{*}P < 0.05$, $^{*}P < 0.01$ compared with non-injured rats (Sham). $^{\#\#}P < 0.01$ compared with the injured control vehicle-treated rats.

positive neurons in the cerebral cortex and dorsal hippocampus (arrows in Fig. 1C) but not in GFAP-positive astrocytes or Iba1-positive microglia as reported previously (Okuma et al., 2012) at the site below percussion 6 h after injury in control rats. No such translocation was observed on the contralateral side in the control rats. In both the cerebral cortex and hippocampus, some neurons had evident cytosolic HMGB1-immunoreactive granule-like structures at 6 h after injury, whereas HMGB1 immunoreactivity disappeared from the other neurons at the primary lesion site.

The administration of GL (4 mg/kg, intravenously) significantly inhibited the translocation of HMGB1 in neurons and maintained the immunoreactivity in the nuclei (Fig. 1C). In accordance with the results of immunohistochemical staining, western blotting revealed that GL suppressed the reduction of HMGB1 from the site of injury (Fig. 1D, E).

Determination of the plasma levels of HMGB1 in rats treated with a percussion intensity of 2.2–2.6 atm showed that an 8-fold increase in HMGB1 levels occurred 6 h after injury. This increase was inhibited by half by intravenous administration of GL (4.0 mg/kg, intravenously) (Fig. 1D).

3.3. Effect of GL on BBB permeability

Evans blue leakage was measured to assess the extravasation of serum albumin from capillary vessels in the TBI model as reported previously (Okuma et al., 2012). The Evans blue dye was injected intravenously 6 h after TBI, and the brain concentrations of Evans blue in the injured hemisphere were determined 3 h thereafter. After fluid percussion injury, the rats received three different doses of intravenous injection of GL (0.25, 1.0 or 4.0 mg/kg) at 5 min. GL dose-dependently inhibited BBB permeability (Fig. 2A, B, C), realizing 43% inhibition at 4.0 mg/kg.

3.4. Real-time PCR of inflammatory molecules

In the previous study, we found a marked up-regulation of inflammation-related molecules including TNF-α and iNOS in the

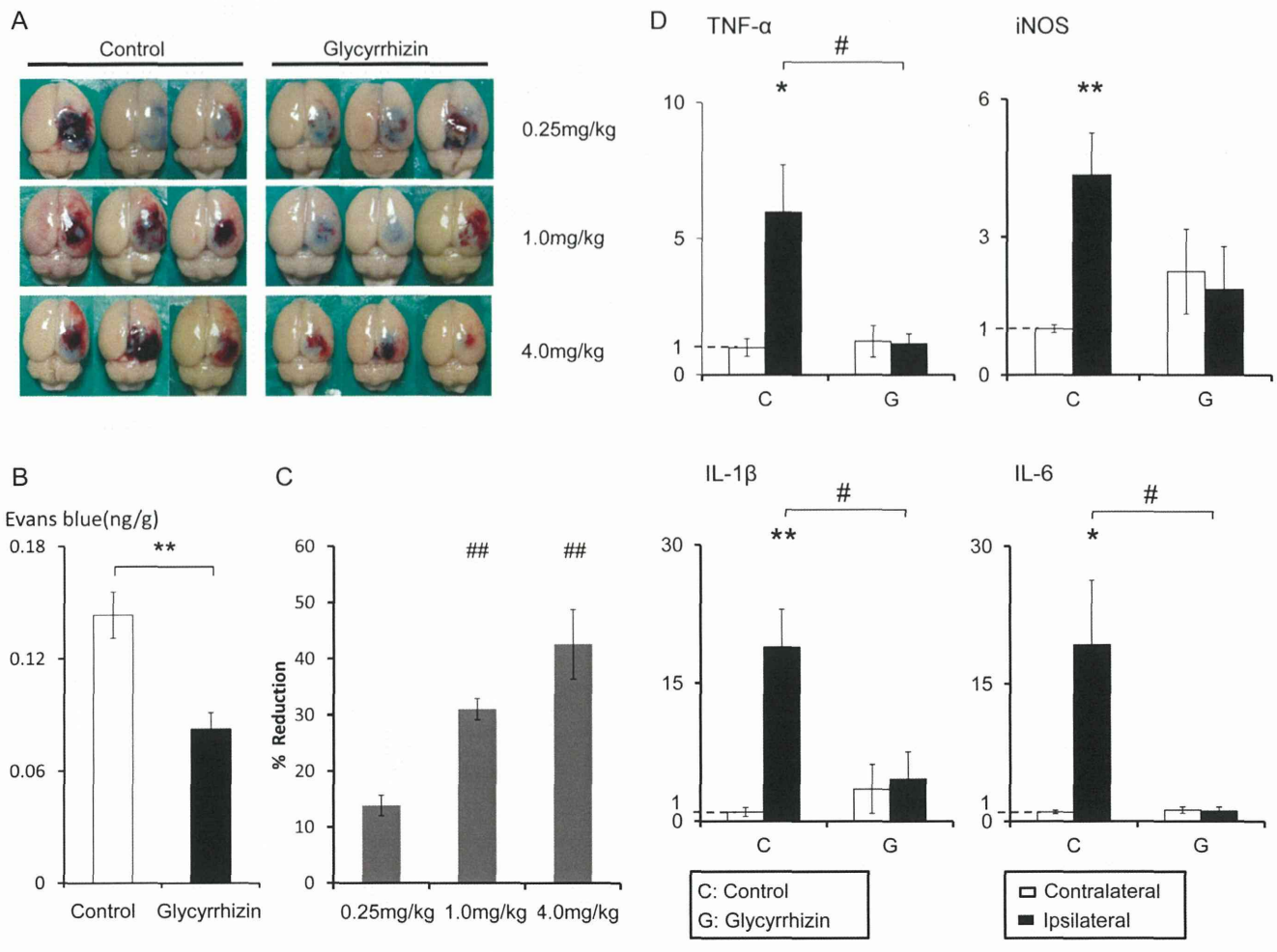

Fig. 2. (A) Effect of GL on BBB permeability in rats with TBI induced by fluid percussion. The rats received intravenous injection of different doses of GL (0.25, 1.0 and 4.0 mg/kg) or control vehicle at 5 min after injury. The permeability of brain capillary vessels was examined by intravenously injecting Evans blue (40 mg/kg) at 6 h after injury and then measuring the leakage of Evans blue-albumin into the brain parenchyma at 3 h after Evans blue injection. (B) After extraction from brain tissue, the amount of Evans blue was determined in both control and GL (4.0 mg/kg) groups. The results are expressed as the mean ± SEM of 5 rats. $^{**}P < 0.01$ compared with the control vehicle-treated rats. (C) The percentage reduction of extravasated Evans blue was calculated in each GL dosage group. $^{\#\#}P < 0.01$ compared with control vehicle-treated rats. (D) Expression of inflammation-related molecules in rats with TBI. The rats received an intravenous injection of GL (4.0 mg/kg) or control vehicle 5 min after injury. Brain samples from both sides of the cerebral cortex were prepared 6 h after injury as described in the Methods section. Real-time quantitative PCR was performed for the determination of inflammation-related molecule expression. The results were normalized to the expression of GAPDH. Results are expressed as the mean ± SEM of 5 rats. $^{*}P < 0.05$, $^{**}P < 0.01$ compared with the contralateral side. $^{\#}P < 0.05$ compared with control rats treated with vehicle.

ipsilateral injured cerebral cortex (Okuma et al., 2012). Therefore, we here examined the effect of GL (4.0 mg/kg) on the expression of inflammatory molecules on both sides of the cerebral cortex using real-time PCR (Fig. 2D). The expression of TNF-α, IL-1β, IL-6 and iNOS was up-regulated in the injured hemisphere after TBI. The treatment with GL (4.0 mg/kg) almost completely suppressed the enhanced expression of TNF-α, IL-1β, and IL-6 in the injured side (Fig. 2D). Also, there was no significant increase in the expression of TNF-α, IL-1β, IL-6 and iNOS in the injured hemisphere in GL-treated rats.

3.5. Effects of GL on motor activity

Impairments of coordinated locomotor activity after percussion injury were evaluated using a rotarod test. The walking time periods before and after brain injury were measured by the rotarod test and were expressed as a ratio of two determinations. In the sham rats, a learning tendency was observed, but this trend did not reach the level of statistical significance. In vehicle control rats, the ratios were significantly reduced compared with sham controls at 3, 6 and 24 h after percussion injury (Fig. 3A). In GL (4.0 mg/kg)-treated rats, there was no difference in the ratios compared with those in the sham rats at 3, 6 or 24 h after injury. Conversely, there were significant differences between the vehicle-treated and GL-treated groups at 6 and 24 h after injury (Fig. 3A). The beneficial effects of GL on coordinated motor activity were dose-dependent when the performance was determined at 6 h after injury (Fig. 3B).

3.6. Lateral dominancy of forelimb movement

Cylinder testing to evaluate the right–left dominancy of forelimb movement showed a time-dependent decrease in contralateral forelimb movement in vehicle control rats, while no lateral

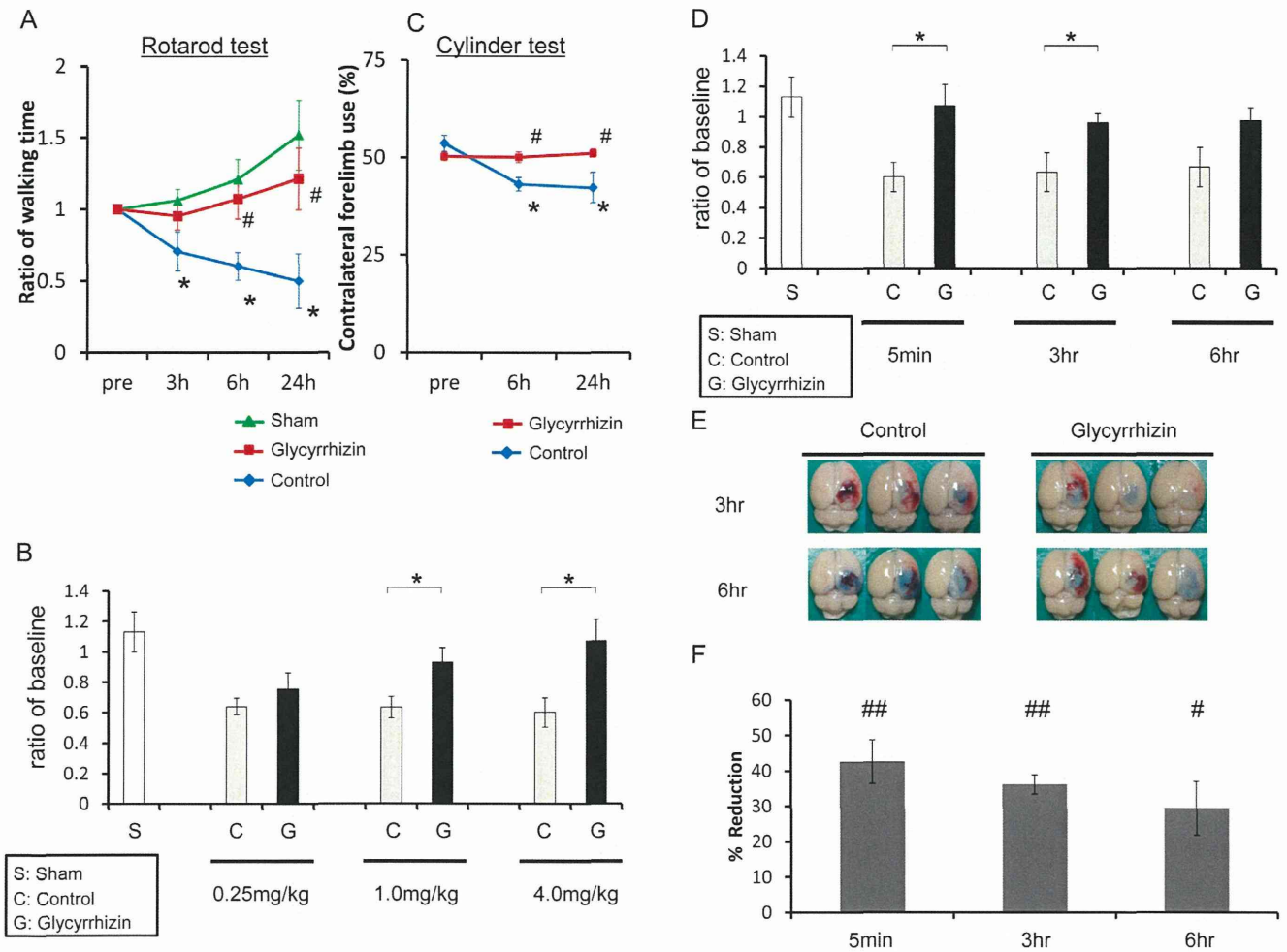

Fig. 3. (A) Effects of GL on the impairment of motor functions in TBI rats. The rats received intravenous injection of GL (4.0 mg/kg) or control vehicle 5 min after injury. The rotarod test was performed before and after TBI on each rat. The results are the ratio of the walking time at each time point against the pre-injured value. The results of the rotarod test were expressed as the mean ± SEM of 5 rats. $^{*}P < 0.05$ compared with the sham control at each time point. $^{\#}P < 0.05$ compared with the corresponding injured control vehicle-treated rats at the same time point. (B) The rats received intravenous injection of different doses of GL (0.25, 1.0 or 4.0 mg/kg) or control vehicle 5 min after injury. The rotarod test was performed at 6 h after injury as in (A). The results were expressed as the mean ± SEM of 5 rats. $^{*}P < 0.05$ compared with the injured control vehicle-treated rats. (C) Effect of GL on the lateral dominance of motor functions in TBI rats. The results of the limb-use asymmetry cylinder test were expressed as the mean ± SEM of 5 rats. $^{*}P < 0.05$ compared with the pretreatment value. $^{\#}P < 0.05$ compared with the injured control vehicle-treated rats. (D) Determination of the therapeutic time window of GL treatment in rat TBI. The rats received intravenous injection of GL (4 mg/kg) or control vehicle at 5 min, 3 h or 6 h after fluid percussion injury. The rotarod test was performed 6 h after injury. Results are expressed as the ratio of the walking time to the pre-injured value. The results are the mean ± SEM of 5 rats. $^{*}P < 0.05$ compared with the injured control rats treated with vehicle. (E) The permeability of brain capillary vessels was examined by intravenously injecting Evans blue (40 mg/kg) at 6 h after injury and then measuring the leakage into the brain parenchyma at 3 h after Evans blue injection. Results for 3 representative individuals are shown. (F) Results are expressed as the percentage reduction of Evans blue content by GL treatment at different time points. The results are the mean ± SEM of 5 rats. $^{*}P < 0.05$, $^{**1}P < 0.01$ compared with injured control rats treated with vehicle.

dominancy of forelimb movement was noted in GL (4.0 mg/kg)-treated rats throughout the observation period (Fig. 3C). There were significant differences between the vehicle-treated and GL-treated groups at both 6 and 24 h after injury.

3.7. Determination of the therapeutic time window of GL

After fluid percussion injury, the rats received intravenous injection of GL (4.0 mg/kg) or vehicle control at 5 min, 3 h or 6 h. Not only at 5 min but also at 3 h, intravenous injection of GL significantly improved the motor impairments as measured by the rotarod test (Fig. 3D). In addition, intravenous administration of GL even at 6 h significantly reduced BBB permeability (Fig. 3E, F). Thus, our data suggested that GL treatment was effective even at 6 h after TBI.

3.8. Evaluation of receptor involvement using gene-knockout mice

In our previous study (Okuma et al., 2012), we demonstrated that RAGE predominantly might mediate the effects of HMGB1 released from neurons in the injured lesion. To confirm the receptors involved, we examined the effects of GL using RAGE−/− and corresponding wild-type mice (Fig. 4A). In the wild-type mice, inhibition of BBB permeability by GL (4.0 mg/kg) treatment was evident, as was observed in the rat experiments. In RAGE−/− mice, the increase in BBB permeability was lower than that in wild-type mice. Treatment of RAGE−/− mice with GL (4.0 mg/kg) did not produce any inhibitory effects on BBB permeability, suggesting that RAGE plays a crucial role in mediating the effects of GL (Fig. 4A). Moreover, GL did not antagonize the motor impairment induced by percussion injury in RAGE−/− mice, although GL significantly ameliorated motor impairment in wild-type mice (Fig. 4B).

3.9. Long-term beneficial effects of GL

The long-term beneficial effects of GL (4.0 mg/kg) were evaluated by the rotarod test at 1, 3 and 7 days after injury (Fig. 5A). In the vehicle-treated rats, the ratio of walking time decreased time-dependently up to 3 days and the reduced ratio remained to 7 days (Fig. 5A). Treatment with GL (4.0 mg/kg) significantly elevated the ratios compared with those in vehicle-treated rats at all time points examined.

We also examined the cognitive and motor function of rats with TBI induced by moderate intensity percussion (2.0–2.2 atm) using a Morris water maze test (Fig. 5B). The swimming time before and after brain injury was measured by the Morris water maze test and expressed as a ratio. In the vehicle control rats, there was marked prolongation of swimming time at 3 and 7 days after injury. In contrast, the swimming time in GL-treated rats at 3 and 7 days was the same as the pre-injury value and significantly different from the vehicle control value.

Long-term observation up to 7 days suggested that GL improves not only coordinated locomotor activity but also cognitive function during the subacute phase of TBI. In accordance with the results of the Morris water maze test and rotarod test, immunohistochemical staining revealed a large number of strong GFAP-positive astrocytes (white arrows in Fig. 5C) with broad processes in the control vehicle-treated rats 7 days after injury in both the cortex and dorsal hippocampus of the injured side (Fig. 5C). The number of these reactive astrocytes was reduced substantially in glycyrrhizin-treated rats.

4. Discussion

In the present study, the results of surface plasmon resonance experiments clearly showed that glycyrrhizin binds to HMGB1, but not to sRAGE, with moderate affinity (Kd value of 4.03 μM). The binding of HMGB1 with sRAGE was inhibited by the addition of glycyrrhizin, with the IC50 value being similar to the Kd value of glycyrrhizin for HMGB1. Thus, glycyrrhizin binding to HMGB1 inhibited HMGB1 binding to sRAGE, leading to the diminution of RAGE signaling. In fact, x-ray crystallographic analysis revealed that GL interacts with the A- and B-box of HMGB1 molecules (Mollica

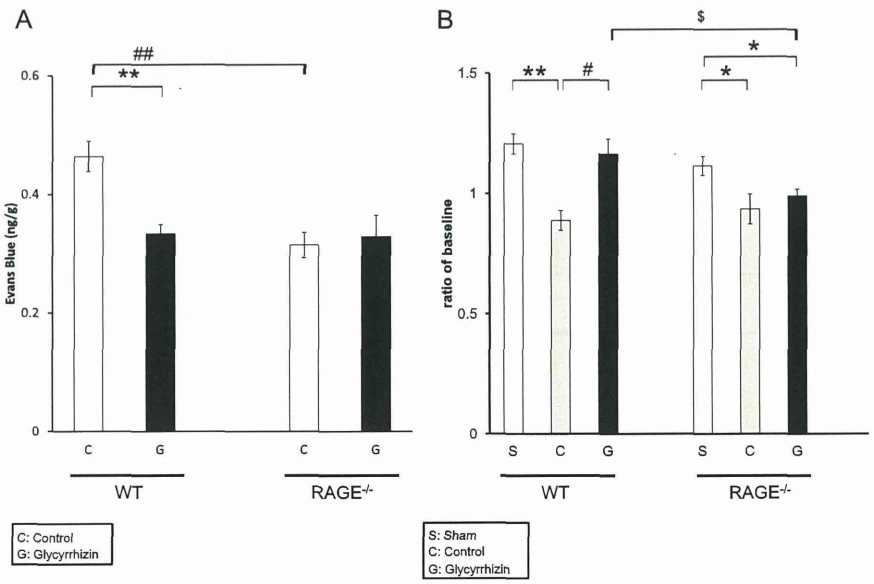

Fig. 4. The effects of GL in RAGE-knockout and wild-type mice. (A) TBI was induced in RAGE−/− and their wild-type mice as described in the Methods section. GL (4.0 mg/kg) or control vehicle was injected at 5 min after percussion injury. BBB permeability was assessed by measuring Evans blue leakage into the brain. Results are expressed as the mean ± SEM of 5 mice. $^{**}P < 0.01$ compared with control mice treated with vehicle. $^{\#\#}P < 0.01$ compared with wild-type (WT) mice. (B) Coordinated motor function was evaluated 6 h after injury using the rotarod test. Results are expressed as the mean ± SEM of 5 mice. $^{*}P < 0.05$, $^{**}P < 0.01$ compared with the respective sham control without injury. $^{\#}P < 0.05$ compared with the respective control mice treated with vehicle. $^{\$}P < 0.05$ compared with wild-type (WT) mice. (For interpretation of the references to color in this figure legend, the reader is referred to the web version of this article.)

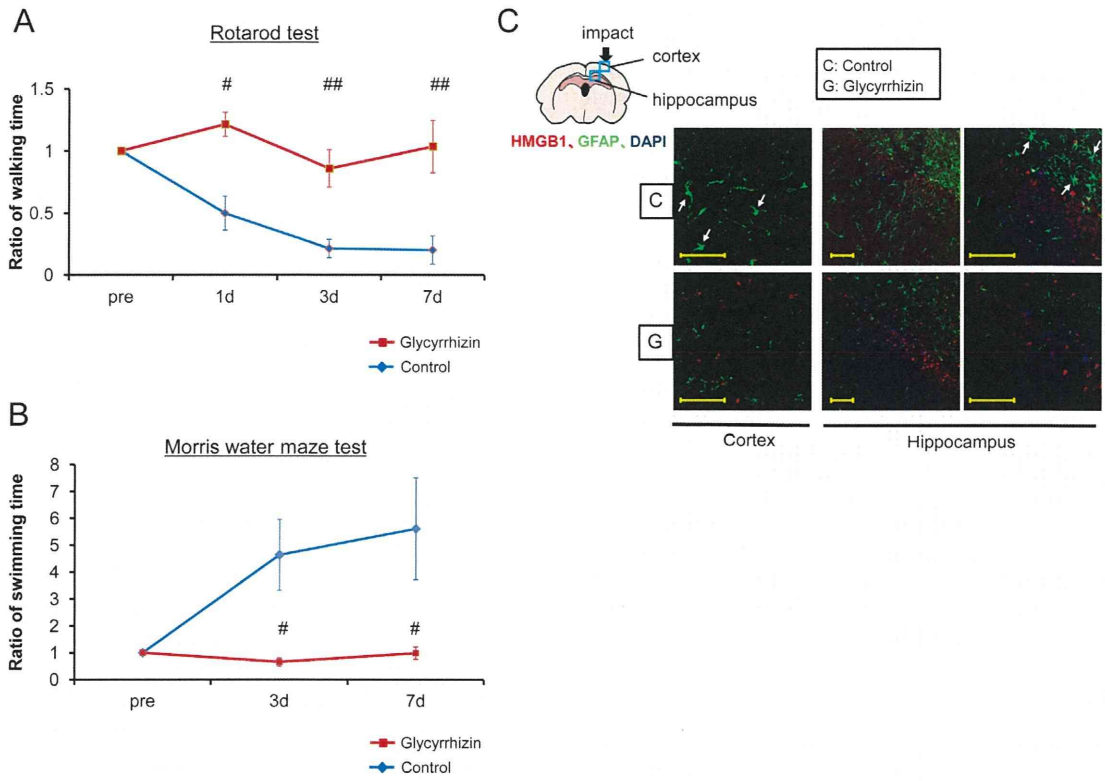

Fig. 5. (A) Long-term beneficial effects of GL on motor activity and cognitive function in TBI rats. The rats received intravenous injection of GL (4.0 mg/kg) or control vehicle at 5 min and at 6 h after fluid percussion injury. Then the same dose of GL was administered once a day for 3 days. The rotarod test was performed at 1, 3 and 7 days after injury. Results are expressed as the mean ± SEM of 6 rats. $^{*}P < 0.05$, $^{**}P < 0.01$ compared with the pre-injured value. $^{\#}P < 0.05$, $^{\#\#}P < 0.01$ compared with injured control rats treated with vehicle. (B) After mild fluid percussion injury, the rats received intravenous injection of GL (4.0 mg/kg) or control vehicle at 5 min and at 6 h. Then the same dose of GL was administered once a day for 3 days. The Morris water maze test was performed before and after mild TBI. Results are expressed as a ratio of swimming time at each time point against the pre-injured value. The results are the mean ± SEM of 6 rats. $^{*}P < 0.05$ compared with the pre-injured value. $^{\#}P < 0.05$ compared with injured control rats treated with vehicle. (C) Immunohistochemical staining of the injured cortex and dorsal hippocampus 7 days after injury. The rats received GL or control vehicle as in (A). The coronal brain sections were double-immunostained with anti-HMGB1 and anti-GFAP antibodies, followed by AlexaFluor 555-labeled and AlexaFluor 488-labeled secondary antibodies, respectively. Nuclei were stained by DAPI. The indicated areas from cerebral cortex and hippocampus CA1 were shown. White arrows indicate the strong GFAP-positive astrocytes. Scale bar = 50 μm.

et al., 2007). Although the amino acid sequence in the B-box has been suggested to be involved in RAGE recognition (Andersson and Tracey, 2011), modification of the A- and B-box by GL may strongly interfere with RAGE binding.

Glycyrrhizin is a major constituent of licorice root that has often been used in traditional medicine in Japan and China (Arase et al., 1997; Kumada, 2002). Injection of glycyrrhizin is available for the treatment of hepatitis and allergic inflammation in Japan. Plural action mechanisms have been suggested for the anti-inflammatory activity of glycyrrhizin, including inhibition of NF-κB activation (Cherng et al., 2006; Takei et al., 2008), suppression of inflammatory cytokine production (Michaelis et al., 2011) and inhibition of the migration of inflammatory cells (Andersson and Tracey, 2011). These effects are interrelated, and some of them may be ascribed to the inhibition of HMGB1 activity and HMGB1 translocation/secretion (Kim et al., 2012; Hwang et al., 2006). The in vivo kinetics of glycyrrhizin indicate that the therapeutic concentration of glycyrrhizin is about 0.4–1.0 μM in humans (Michaelis et al., 2011; Van Rossum et al., 1999), which is close to the Kd value of glycyrrhizin binding to HMGB1 determined in the present study. Therefore, a routine dose of glycyrrhizin (40 mg/injection) may yield sufficient plasma levels of glycyrrhizin to interfere with HMGB1–RAGE binding.

We observed a marked translocation of HMGB1 in pyramidal neurons in both the cerebral cortex and CA1 hippocampus under percussion injury (Fig. 1C). The reduced HMGB1 levels detected by western blotting in the injured cerebral cortex (Fig. 1D, E) strongly suggested that the rate of translocation and release of HMGB1 from neuronal nuclei into extracellular space exceeded substantially that of synthesis in the injury core. As in the case of anti-HMGB1 monoclonal antibody treatment (Okuma et al., 2012), glycyrrhizin significantly inhibited the translocation of HMGB1 in neurons (Fig. 1C). This strongly suggested the existence of a cycle in which HMGB1 is released, and then induces its own translocation, leading to further HMGB1 release, that was inhibited by glycyrrhizin. Since glycyrrhizin inhibited HMGB1 and sRAGE binding, it was speculated that inhibition of RAGE signaling may in turn lead to the suppression of HMGB1 translocation by GL. Thus, the direct binding of GL to HMGB1 and subsequent inhibition of HMGB1 translocation support the notion that GL may be an inhibitor of HMGB1 secretion (Kim et al., 2012; Gong et al., 2012; Ohnishi et al., 2011).

Glycyrrhizin therapy is considered to be rather safe due to its long clinical experience of use. Pseudo-aldosteronism is the sole major side effect of glycyrrhizin and is generally limited to cases requiring long-term treatment. In the present study, two administrations of glycyrrhizin at 5 min and at 6 h after injury achieved a greater than 90% inhibition of the expressions of TNF-α, IL-1β, and IL-6. These anti-inflammatory effects of glycyrrhizin and inhibition of HMGB1 mobilization suggested by immunohistochemical study

as well as reduction of plasma levels of HMGB1 probably contributed to the protection of the blood–brain barrier (BBB), since in vitro experiments showed that HMGB1 induced a breakdown of the BBB directly (Zhang et al., 2011). Thus, glycyrrhizin inhibited BBB breakdown, expression of inflammation-related cytokines and elevation of plasma levels of HMGB1, probably through its binding to HMGB1, which would have downregulated the RAGE signaling pathway. In fact, the beneficial effects of glycyrrhizin disappeared in RAGE-knockout mice in the present study.

The beneficial effects of glycyrrhizin on sensorimotor and cognitive functions continued for up to at least 7 days after injury. The numbers of reactive astrocytes in the lesion site were reduced in glycyrrhizin-treated rats. Therefore, it is speculated that the acute effects of glycyrrhizin on BBB disruption as well as expression of inflammation-related molecules were followed by a reduced activation of astrocytes. One of the major complications of traumatic brain injury is post-traumatic epilepsy. Since the epileptic foci probably exhibits the sustained activation of astrocytes and microglia (Pascual et al., 2012; Zurolo et al., 2011; Mattson and Camandola, 2001), the reduced activation of astrocytes and microglia may lead to a reduction in the severity of epileptic status. Because of the absence of severe side effects, glycyrrhizin may be applicable for the treatment of traumatic brain injury and prevention of post-traumatic epilepsy.

5. Conclusion

It was demonstrated that GL exerts beneficial effects on acute traumatic brain injury as well as subacute neural functions through binding to HMGB1 and interference with its RAGE ligation. Glycyrrhizin has long been used in the clinic setting and is a safe drug. Therefore, a clinical study evaluating the efficacy of GL on TBI should be considered.

Acknowledgments

This work was supported by grants from the Scientific Research from the Ministry of Health, Labor and Welfare of Japan, from the Japan Society for the Promotion of Science (JSPS No. 23659687, 24390061).

References

Andersson, U., Tracey, K.J., 2011. HMGB1 is a therapeutic target for sterile inflammation and infection. Annu. Rev. Immunol. 29, 139–162.
Arase, Y., Ikeda, K., Murashima, N., Chayam, K., Tsubota, A., Koida, I., Suzuki, Y., Saitoh, S., Kobayashi, M., Kumada, H., 1997. The long term efficacy of glycyrrhizin in chronic hepatitis C patients. Cancer 79, 1494–1500.
Cherng, J.M., Lin, H.J., Hung, M.S., Lin, Y.R., Chan, M.H., Lin, J.C., 2006. Inhibition of nuclear factor κB is associated with neuroprotective effects of glycyrrhizic acid on glutamate-induced excitotoxocity in primary neurons. Eur. J. Pharmacol. 547, 10–21.
Gong, G., Yuan, L.B., Hu, L., Wu, W., Yin, L., Hou, J.L., Liu, Y.H., Zhou, L.S., 2012. Glycyrrhizin attenuates rat ischemic spinal cord injury by suppressing inflammatory cytokines and HMGB1. Acta Pharmacol. Sin. 33, 11–18.
He, M., Kubo, H., Morimoto, K., Fujino, N., Suzuki, T., Takahasi, T., Yamada, M., Yamaya, M., Maekawa, T., Yamamoto, Y., Yamamoto, H., 2011. Receptor for advanced glycation end products binds to phosphatidyl serine and assists in the clearance of apoptotic cells. EMBO Rep. 12, 358–364.
Hidaka, I., Hino, K., Korenaga, M., Gondo, T., Nishina, S., Ando, M., Okuda, M., Sakaida, I., 2007. Stronger Neo-Minophagen C, a glycyrrhizin-containing preparation, protects liver against carbon tetrachloride-induced oxidative stress in transgenic mice expressing the hepatitis C virus polyprotein. Liver Int. 27, 845–853.
Hwang, I.K., Lim, S.S., Choi, K.H., Yoo, K.Y., Shin, H.K., Kim, E.J., Yoon-Park, J.H., Kang, T.C., Kim, Y.S., Kwon, D.Y., Kim, D.W., Moon, W.K., Won, M.H., 2006. Neuroprotective effects of roasted licorice, not raw form, on neuronal injury in gerbil hippocampus after transient forebrain ischemia. Acta Pharmacol. Sin. 27, 959–965.
Kim, S.W., Jin, Y., Shin, J.H., Kim, I.D., Lee, H.K., Park, S., Han, P.L., Lee, J.K., 2012. Glycyrrhizic acid affords robust neuroprotection in the postischemic brain via anti-inflammatory effect by inhibiting HMGB1 phosphorylation and secretion. Neurobiol. Dis. 46, 147–156.
Kumada, H., 2002. Long-term treatment of chronic hepatitis C with glycyrrhizin [stronger neo-minophagen C (SNMC)] for preventing liver cirrhosis and hepatocellular carcinoma. Oncology 62, 94–100.
Liu, K., Mori, S., Takahashi, H.K., Tomono, Y., Wake, H., Kanke, T., Sato, Y., Hiraga, N., Adachi, N., Yoshino, T., Nishibori, M., 2007. Anti-high mobility group box 1 monoclonal antibody ameliorates brain infarction induced by transient ischemia in rats. FASEB J. 21, 3904–3916.
Liu, R., Mori, S., Wake, H., Zhang, J., Liu, K., Izushi, Y., Takahashi, H.K., Peng, B., Nishibori, M., 2009. Establishment of in vitro binding assay of high mobility group box-1 and S100A12 to receptor for advanced glycation end products: heparin's effect on binding. Acta Med. Okayama 63, 203–211.
Lotze, M.T., Tracey, K.J., 2005. High-mobility group box1 protein (HMGB1): nuclear weapon in the immune arsenal. Nat. Rev. Immunol. 5, 331–342.
Mabuchi, A., Wake, K., Marlini, M., Watanabe, H., Wheatley, A.M., 2009. Protection by glycyrrhizin against warm ischemia-reperfusion-induced cellular injury and derangement of the microcirculatory blood flow in the rat liver. Microcirculation 16, 364–376.
Mattson, M.P., Camandola, S., 2001. NF-kappaB in neuronal plasticity and neurodegenerative disorders. J. Clin. Investig. 107, 247–254.
Michaelis, M., Geiler, J., Naczk, P., Sithisarn, P., Leutz, A., Doerr, H.W., Cinatl Jr., J., 2011. Glycyrrhizin exerts antioxidative effects in H5N1 influenza A virus-infected cells and inhibits virus replication and pro-inflammatory gene expression. PLoS One 6, e19705.
Miyaji, C., Miyakawa, R., Watanabe, H., Kawamura, H., Abo, T., 2002. Mechanisms underlying the activation of cytotoxic function mediated by hepatic lymphocytes following the administration of glycyrrhizin. Int. Immunopharmacol. 2, 1079–1086.
Mollica, L., De Marchis, F., Spitaleri, A., Dallacosta, C., Pennacchini, D., Zamai, M., Agresti, A., Trisciuoglio, L., Musco, G., Bianchi, M.E., 2007. Glycyrrhizin binds to high-mobility group box 1 protein and inhibits its cytokine activities. Chem. Biol. 14, 431–441.
Morris, R., 1984. Developments of a water-maze procedure for studying spatial learning in the rat. J. Neurosci. Methods 11, 47–60.
Myint, K.M., Yamamoto, Y., Doi, T., Kato, I., Harashima, A., Yonekura, H., Watanabe, T., Shinohara, H., Takeuchi, M., Tsuneyama, K., Hashimoto, N., Asano, M., Takasawa, S., Okamoto, H., Yamamoto, H., 2006. RAGE control of diabetic nephropathy in a mouse model. Effects of RAGE gene disruption and administration of low-molecular weight heparin. Diabetes 55, 2510–2522.
Narayan, R.K., Michel, M.E., Ansell, B., Baethmann, A., Biegon, A., Bracken, M.B., Bullock, M.R., Choi, S.C., Clifton, G.L., Contant, C.F., Coplin, W.M., Dietrich, W.D., Ghajar, J., Grady, S.M., Grossman, R.G., Hall, E.D., Heetderks, W., Hovda, D.A., Jallo, J., Katz, R.L., Knoller, N., Kochanek, P.M., Maas, A.I., Majde, J., Marion, D.W., Marmarou, A., Marshall, L.F., McIntosh, T.K., Miller, E., Mohberg, N., Muizelaar, J.P., Pitts, L.H., Quinn, P., Riesenfeld, G., Robertson, C.S., Strauss, K.I., Teasdale, G., Temkin, N., Tuma, R., Wade, C., Walker, M.D., Weinrich, M., Whyte, J., Wilberger, J., Young, A.B., Yurkewicz, L., 2002. Clinical trial in head injury. J. Neurotrauma 19, 503–557.
Ohnishi, M., Katsuki, H., Fukutomi, C., Takahashi, M., Motomura, M., Fukunaga, M., Matsuoka, Y., Isohama, Y., Izumi, Y., Kume, T., Inoue, A., Akaike, A., 2011. HMGB1 inhibitor glycyrrhizin attenuates intracerebral hemorrhage-induced injury in rats. Neuropharmacology 61, 975–980.
Ohshima, T., Ogura, H., Tomizawa, K., Hayashi, K., Suzuki, H., Saito, T., Kamei, H., Nishi, A., Bibb, J.A., Hisanaga, S., Matsui, H., Mikoshiba, K., 2005. Impairment of hippocampal long-term depression and defective spatial learning and memory in p35 mice. J. Neurochem. 94, 917–925.
Okuma, Y., Liu, K., Wake, H., Zhang, J., Maruo, T., Date, I., Yoshino, T., Ohtsuka, A., Otani, N., Tomura, S., Shima, K., Yamamoto, Y., Yamamoto, H., Takahashi, H.K., Mori, S., Nishibori, M., 2012. Anti-high mobility group box-1 antibody therapy for traumatic brain injury. Ann. Neurol. 72, 373–384.
Otani, N., Nawashiro, H., Fukui, S., Nomura, N., Shima, K., 2002. Temporal and spatial profile of phosphorylated mitogen-activated protein kinase pathways after lateral fluid percussion injury in the cortex of the rat brain. J. Neurotrauma 19, 1587–1596.
Pascual, O., Ben Achour, S., Rostaing, P., Triller, A., Bessis, A., 2012. Microglia activation triggers astrocyte-mediated modulation of excitatory neurotransmission. Proc. Natl. Acad. Sci. U. S. A. 109, E197–E205.
Schiraldi, M., Raucci, A., Muñoz, L.M., Livoti, E., Celona, B., Venereau, E., Apuzzo, T., De Marchis, F., Pedotti, M., Bachi, A., Thelen, M., Varani, L., Mellado, M., Proudfoot, A., Bianchi, M.E., Uguccioni, M., 2012. HMGB1 promotes recruitment of inflammatory cells to damaged tissues by forming a complex with CXCL12 and signaling via CXCR4. J. Exp. Med. 209, 551–563.
Shamsa, F., Ohtsuki, K., Hasanzadeh, E., Rezazadeh, S.h, 2010. The anti-inflammatory and anti-viral effects of an ethnic medicine: glycyrrhizin. J. Med. Plants 9, 1–28.
Sharifzadeh, M., Shamsa, F., Shiran, S., Karimfar, M.H., Miri, A.H., Jalalizadeh, H., Gholizadeh, S., Salar, F., Tabrizian, K., 2008. A time course analysis of systemic administration of aqueous licorice extract on spatial memory retention in rats. Planta Med. 74, 485–490.
Shlosberg, D., Benifla, M., Kaufer, D., Friedman, A., 2010. Blood–brain barrier breakdown as a therapeutic target in traumatic brain injury. Nat. Rev. Neurol. 6, 393–403.
Takei, H., Baba, Y., Hisatsune, A., Katsuki, H., Miyata, T., Yokomizo, K., Isohama, Y., 2008. Glycyrrhizin inhibits interleukin-8 production and nuclear factor-κB

activity in lung epithelial cells, but not through glucocorticoid receptors. J. Pharmacol. Sci. 106, 460–468.
Van Rossum, T.G., Vulto, A.G., Hop, W.C., Schalm, S.W., 1999. Pharmacokinetics of intravenous glycyrrhizin after single and multiple doses in patients with chronic hepatitis C infection. Clin. Ther. 21, 2080–2090.
Zhang, J., Takahashi, H.K., Liu, K., Wake, H., Liu, R., Maruo, T., Date, I., Yoshino, T., Ohtsuka, A., Mori, S., Nishibori, M., 2011. Anti-high mobility group box-1 monoclonal antibody protects the blood–brain barrier from ischemia-induced disruption in rats. Stroke 42, 1420–1428.
Zurolo, E., Iyer, A., Maroso, M., Carbonell, C., Anink, J.J., Ravizza, T., Fluiter, K., Spliet, W.G., van Rijen, P.C., Vezzani, A., Aronica, E., 2011. Activation of toll-like receptor, RAGE and HMGB1 signaling in malformations of cortical development. Brain 134, 1015–1032.

*The Journal of Laryngology & Otology (2014), **128**, 926–931.*
© JLO (1984) Limited, 2014
doi:10.1017/S0022215114001819

MAIN ARTICLE

Does HMGB1 predict occult neck lymph node metastasis in early tongue carcinoma? A case–control study of 26 patients

H HANAKAWA[1], Y ORITA[1], Y SATO[2], M TAKEUCHI[2], S TAKAO[3], K OHNO[2], T KOHNO[1], N IWAKI[2], H MARUNAKA[4], R TAMAMURA[5], M NISHIBORI[6], H NAGATSUKA[5], K NISHIZAKI[1], T YOSHINO[2]

Departments of [1]Otolaryngology Head and Neck Surgery, [2]Pathology, [3]Epidemiology, [5]Oral Pathology and Medicine, and [6]Pharmacology, Okayama University Graduate School of Medicine, Dentistry and Pharmaceutical Sciences, and [4]Department of Otolaryngology Head and Neck Surgery, Okayama Medical Center, Japan

Abstract

Objective: This study examined whether the occurrence of late neck metastasis in early tongue squamous cell carcinoma can be predicted by evaluating HMGB1 (high mobility group box 1) expression in the primary lesion.

Methods: A case–control study was conducted. The cases comprised 10 patients with late neck metastasis. The controls consisted of 16 patients without recurrence. All were examined immunohistochemically for HMGB1 protein expression. The odds ratio for late neck metastasis in relation to HMGB1 was estimated.

Results: Results for HMGB1 were dichotomised into positive staining scores (score, 5–7) and negative scores (0–4). Six cases (60 per cent) and four controls (25 per cent) were HMGB1-positive. Although no significant result was seen, compared with HMGB1-negative patients the odds ratio for late neck metastasis in HMGB1-positive patients was 3.8 (95 per cent confidence interval, 0.6–26.5) after adjusting for other factors.

Conclusion: In the present study, immunohistochemical study of HMGB1 in early tongue squamous cell carcinoma did not appear to be very useful for predicting occult neck metastasis. Further study is necessary to clarify the relationship between HMGB1 expression and late neck metastasis in early tongue squamous cell carcinoma.

Key words: HMGB1; Tongue; Carcinoma; Metastasis

Introduction

The clinical course of early tongue carcinoma is difficult to predict using established risk factors. We sometimes encounter cases with a poor prognosis among patients who initially show a very superficial pathologically staged primary tumour (T_1), without clinical evidence of metastatic disease. The presence or absence of occult neck metastasis is one of the major prognostic factors in node-negative (N_0) tongue carcinoma.[1] The prevalence of occult neck metastasis among patients with early tongue carcinoma is estimated to be about 20–30 per cent. Several studies have addressed the need for prophylactic neck dissection in patients with clinically staged N_0 early tongue carcinoma (tumour–node–metastasis (TNM) staging of $T_{1/2}$ N_0M_0).[2]

In Japan, many facilities employ a wait-and-see strategy for patients with clinical N_0 tongue carcinoma after close pre-operative image diagnosis. This is in light of the burden on the patient, and the risk of surgical complications such as palsy of the mandibular branch of the facial nerve and shoulder dysfunction.[3] As the Japanese medical insurance system allows all patients easy access to hospitals and frequent, careful follow up, immediate neck dissection can be performed shortly after neck metastasis is detected. However, the survival rate of patients with late metastasis is not high.[1,4] Depth of tumour invasion is the most widely accepted predictor of late metastasis,[1,5,6] but much room remains for evaluating prognosis more precisely.[7,8]

HMGB1 (high mobility group box 1), a chromatin-associated nuclear protein, is constitutively expressed in the nucleus of both cancer and normal cells. HMGB1 overexpression has been reported in a variety of human cancers, and has been identified as a general regulator of cell migration.[9] HMGB1 protein is claimed to affect cell invasion, tumour growth and metastasis by high-affinity binding to

Presented at the 37th annual meeting of the Japan Head and Neck Cancer Society, 13–14 June 2013, Tokyo, Japan.
Accepted for publication 25 January 2014 First published online 17 September 2014

RAGE (receptor for advanced glycation end-products).[10] Previous studies have observed expression of HMGB1 in various stages of cancer, or have compared expression of HMGB1 in cancer with expression in normal tissues. The information that expression levels of HMGB1 are significantly higher in cancers than in normal tissues, or are significantly correlated with clinical stage or pathological grade of cancers, so far does not seem very useful for clinicians. However, HMGB1 might offer a target for treatment in cancer based on the inhibition of tumour cell invasion.[9,10]

The present study examined expression of HMGB1 in tongue squamous cell carcinoma (SCC), limited to the early stages (stage I or II according to the Union for International Cancer Control staging criteria), to demonstrate whether this factor can be used to predict the occurrence of late neck metastasis.

Materials and methods

Patients

Paraffin-embedded samples were obtained from 26 stage I or II primary tongue SCC patients (according to the Union for International Cancer Control staging criteria). Diagnoses in these 26 patients had previously been confirmed by physical examination, ultrasonography, computed tomography with or without ^{18}F-deoxyglucose positron emission tomography, and histological examination. If neck metastasis was suspected based on any of these preliminary examinations, ultrasound-guided fine needle aspiration cytology was performed to confirm a negative result. All specimens were obtained from patients who underwent partial glossectomy at Okayama University Hospital, Japan, without any other treatments, including prophylactic neck dissection, pre- or post-operative chemotherapy, or radiotherapy.

The cases comprised 10 patients who were treated between January 2005 and March 2012, and were found to have neck metastasis during follow up. The sites of late neck metastases were level 1 in two cases, level 2 in five, both levels 1 and 2 in two, and level 3 in one, respectively. The controls consisted of 16 patients who were treated between January 2005 and March 2008, and had been observed without recurrence for more than 5 years, thus being considered as having achieved complete cure. None of the 26 patients developed local recurrence or distant metastasis, and none were lost to follow up during the observation period.

Immunohistochemical staining

Serial sections (4 μm) were cut from each paraffin-embedded tissue block, and several sections were stained with haematoxylin and eosin. The sections were immunohistochemically stained with rat monoclonal anti-HMGB-1 antibody (10 μg/ml) using an automated Bond-Max stainer (Leica Biosystems, Melbourne, Australia). The anti-HMGB-1 antibody was provided by a pharmacologist.[11]

Staining evaluation

Immunohistochemically stained tissue sections were scored separately by three pathologists blinded to the clinical parameters. HMGB1 staining was mostly observed in the nuclei and cytoplasm of carcinoma cells and some fibroblasts. Staining intensity was scored as: 0 = negative, 1 = weak, 2 = medium or 3 = strong (Figure 1). The extent of staining to the entire carcinoma-involved area was scored as: 0 = 0 per cent, 1 = 1–25 per cent, 2 = 26–50 per cent, 3 = 51–75 per cent or 4 = 76–100 per cent. The sum of the intensity and extent scores was used as the final staining score (0–7) for HMGB1.[12] This grading system has previously been used for evaluation of HMGB1 expression in the immunohistochemically stained tissue sections of nasopharyngeal carcinoma.[12] After deciding on the scores independently, the three pathologists gathered to discuss appropriate scores and decide on the final scores. Patients were then categorised as HMGB1-positive (HMGB1 score = 5–7) or HMGB1-negative (HMBG1 score = 0–4).

Statistical analysis

We first assessed univariate associations between demographic characteristics and potential prognostic factors including HMGB1 expression and late neck metastasis. Crude odds ratios were then estimated. Logistic regression modelling was used to examine associations between HMGB1 and late neck metastasis, adjusting for other prognostic factors. Adjusted variables were selected for inclusion in the model on the bases of both the strength of the association and clinical importance. Odds ratios and 95 per cent confidence intervals (CIs) were calculated. Values of $p < 0.05$ (two-sided test) were considered statistically significant. All analyses were performed using SPSS version 21.0 J software (SPSS, Armonk, New York, USA) and STATA/SE 12.0 J software (Stata, College Station, Texas, USA).

Results

Of the 26 tongue SCC patients (Table I), 11 were female and 15 were male (57.7 per cent males), ranging in age from 29 to 87 years (median, 63 years; mean, 69 years). The primary site for all 26 patients was the edge of the tongue, with no cases showing the primary lesion at the centre or root of the tongue. All 26 patients underwent partial glossectomy without prophylactic neck dissection. Pathological study revealed that all the specimens were completely resected with sufficient margins. Of the 10 patients with late neck metastases, 8 survived and 2 died of the disease during the observation period. The interval between surgery for primary tongue carcinoma and presentation of neck metastases ranged from 3 to 18 months (mean, 8.5 months).

As summarised in Table II, no significant associations were seen between late neck metastases in early

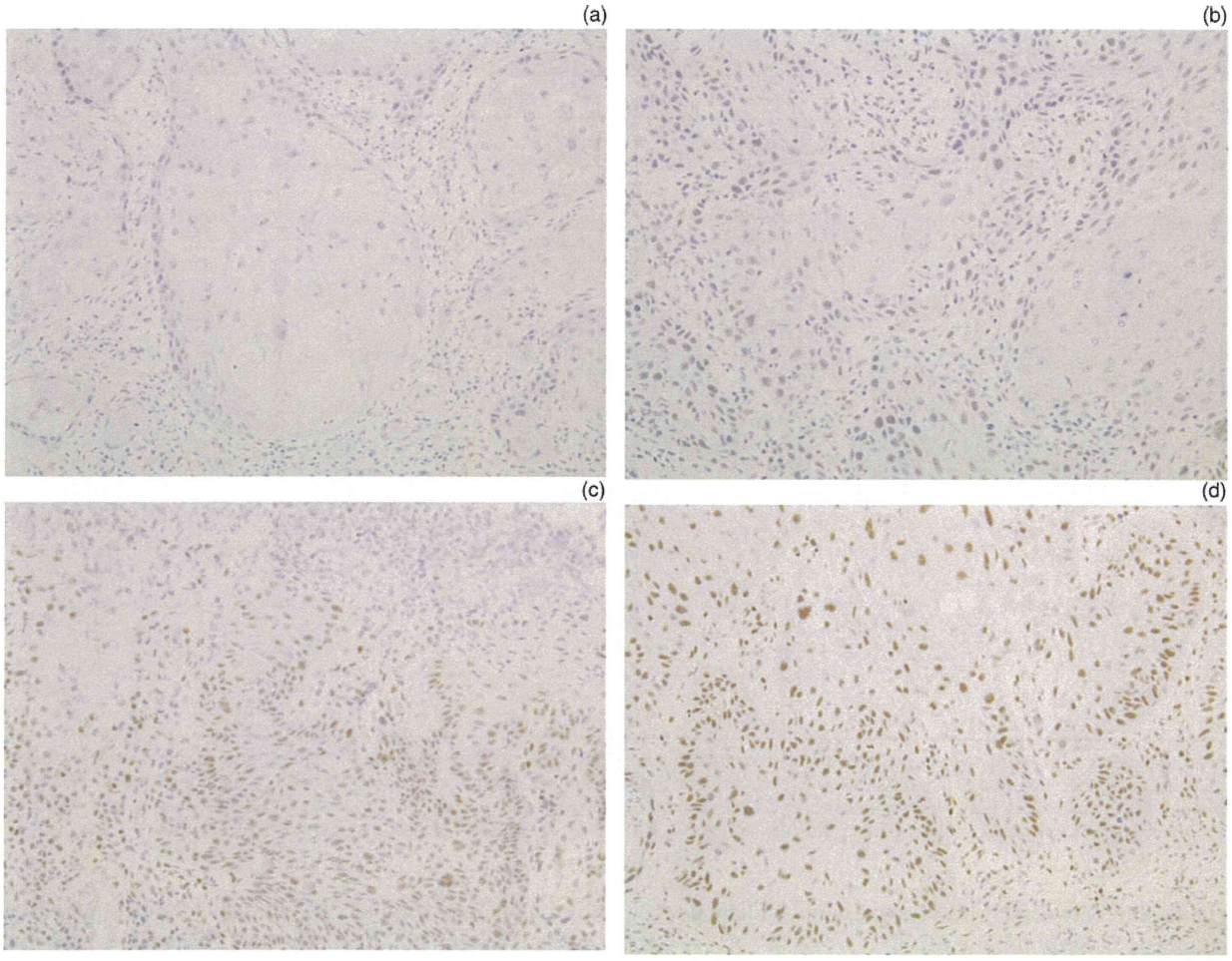

FIG. 1

HMGB1 expression in early tongue squamous cell carcinoma. Immunohistochemical staining intensity with HMGB1 antibody was scored as: 0 = negative (a), 1 = weak (b), 2 = moderate (c) or 3 = strong (d). (×200)

tongue carcinoma and sex, age, tumour classification (T_1 or T_2), pathological differentiation, or HMGB1 expression (positive *vs* negative). However, the point estimate of HMGB1 expression was 4.50 and indicated a relatively strong association.

Table III shows the adjusted odds ratios and 95 per cent CIs for HMGB1 and selected variables. As this study included only a small number of patients ($n = 26$), analysis of many of the prognostic factors by multivariate analyses in the same model might be imprecise and problematic. Based on both the strength of the associations and clinical importance, we selected sex as a demographic variable and tumour classification as a clinical characteristic for adjusting the relationship between HMGB1 and late neck metastasis. The adjusted odds ratio for positive HMGB1 (HMBG1 score of 5–7) was 3.82 (95 per cent CI, 0.55–26.50) compared with negative HMGB1 (HMBG1 score of 0–4).

Discussion

Our findings indicate that HMGB1 might not be useful as a predictive marker for late neck metastasis in early tongue SCC compared with previously established risk factors. Two possible explanations for our findings were considered: (1) HMGB1 is truly a prognostic marker, or (2) HMGB1 is a confounder that needs to be adjusted for when estimating associations with other potential predictors. As the point estimate showed a relatively strong association per se, HMGB1 might still be identified as a significant prognostic factor in a future study with more statistical power (i.e. many more patients). In addition, the odds ratios of sex and tumour stage T_2 were obviously increased after adjusting for HMGB1 in the same model. This might suggest HMGB1 as a possible confounder in determining relationships between other prognostic factors and late neck metastasis. The scoring system used for the evaluation of HMGB1 staining has been employed in previous studies.[12,13] In a study of HMGB1 expression in oesophageal SCC, the total staining score of HMGB1 was calculated by multiplying the intensity and extent scores.[14] We also used this calculation method to analyse the data, and attained almost the same results. It will be necessary to accumulate more cases to clarify the